ORIGINAL RESEARCH

New Function of RUNX2 in Regulating Osteoclast Differentiation via the AKT/NFATc1/CTSK Axis

Yuejiao Xin[1] · Yang Liu[1] · Dandan Liu[1] · Jie Li[1] · Chenying Zhang[1] · Yixiang Wang[2] · Shuguo Zheng[1]

Abstract
Cleidocranial dysplasia is an autosomal dominant skeletal disorder resulting from RUNX2 mutations. The influence of RUNX2 mutations on osteoclastogenesis and bone resorption have not been reported. To investigate the role of RUNX2 in osteoclast, RUNX2 expression in macrophages (RAW 264.7 cells) was detected. Stable RAW 264.7 cell lines expressing wild-type RUNX2 or mutated RUNX2 (c.514delT, p.172 fs) were established, and their functions in osteoclasts were investigated. Wild-type RUNX2 promoted osteoclast differentiation, formation of F-actin ring, and bone resorption, while mutant RUNX2 attenuated the positive differentiation effect. Wild-type RUNX2 increased the expression and activity of mTORC2. Subsequently, mTORC2 specifically promoted phosphorylation of AKT at the serine 473 residue. Activated AKT improved the nuclear translocation of NFATc1 and increased the expression of downstream genes, including CTSK. Inhibition of AKT phosphorylation abrogated the osteoclast formation of wild-type macrophages, whereas constitutively activated AKT rescued the osteoclast formation of mutant macrophages. The present study suggested that RUNX2 promotes osteoclastogenesis and bone resorption through the AKT/NFATc1/CTSK axis. Mutant RUNX2 lost the function of regulating osteoclast differentiation and bone remodeling, resulting in the defective formation of the tooth eruption pathway and impaction of permanent teeth in cleidocranial dysplasia. This study, for the first time, verifies the effect of RUNX2 on osteoclast differentiation and bone resorption and provides new insight for the explanation of cleidocranial dysplasia.

Keywords Cleidocranial dysplasia · RUNX2 mutation · Osteoclast differentiation · AKT/NFATc1/CTSK axis

✉ Yixiang Wang
kqwangyx@bjmu.edu.cn

✉ Shuguo Zheng
kqzsg86@bjmu.edu.cn

1   Department of Preventive Dentistry, Peking University School and Hospital of Stomatology & National Clinical Research Center for Oral Diseases & National Engineering Laboratory for Digital and Material Technology of Stomatology & Beijing Key Laboratory of Digital Stomatology, Beijing, People's Republic of China

2   Central Laboratory, Department of Oral and Maxillofacial Surgery, Peking University School and Hospital of Stomatology & National Clinical Research Center for Oral Diseases & National Engineering Laboratory for Digital and Material Technology of Stomatology & Beijing Key Laboratory of Digital Stomatology, Beijing, People's Republic of China

Introduction

Cleidocranial dysplasia (CCD; MIM 119,600) is an autosomal dominant disorder. Runt-related transcription factor-2 (RUNX2) mutations cause CCD and can be detected in about 70% of CCD patients [1]. Typical clinical features of CCD involve skeletal hypoplasia and dental anomalies. The former includes delayed closing of fontanelle, hypoplastic clavicles, brachycephalic skull, frontal bossing, and short stature and the latter refers to supernumerary teeth, retention of deciduous teeth, and impaction of permanent teeth [2–4]. In mixed dentition, conspicuous delayed eruption of permanent teeth, which affects masticatory function and facial development, usually becomes the significant reason that patients receive oral examination and are diagnosed with CCD.

Bone formation and bone resorption are both required in tooth eruption [5–7]. Bone resorption overlying the permanent tooth germ forms the eruption pathway [8], and bone formation at the base of the tooth germ provides the

motive force for eruption [9]. These two biological processes contribute to successful eruption of the tooth. Disturbed permanent tooth eruption in CCD patients is related to an imbalance between bone formation and bone resorption. Although numerous studies have described the etiological mechanism of CCD, mainly focusing on osteoblastic dysfunction (including the osteoclast-inductive ability) and impaired bone formation [10–12], the direct impacts of osteoclastic disorder and reduced bone resorption have not been reported.

Osteoclasts (OCs) are derived from hematopoietic stem cells or monocytes/macrophage progenitor cells, and they are mainly responsible for bone resorption in bone remodeling [13]. Receptor activator of nuclear factor kappa B ligand (RANKL) [14] is one of the most important factors in regulation of osteoclastogenesis [15]. Osteoblasts mediate the differentiation, maturation, and activation of OCs through various cytokines including RANKL [16]. RUNX2 modulates osteoclast differentiation by controlling the expression of RANKL and osteoprotegerin (OPG) [17–19]. Nevertheless, previous studies have not reported whether RUNX2 mutations influence the internal signaling pathways of osteoclasts.

In the present, the impact of study RUNX2 mutations on osteoclast differentiation and bone resorption was explored to explain the molecular mechanism of delayed permanent tooth eruption in CCD from a new point of perspective.

Materials and Methods

Participants

A 20-year-old man, diagnosed with CCD according to clinical features and genetic analysis, and three gender- and age-matched healthy controls were included in the present study with informed consent [20]. Ethical approval for this study was obtained from the Ethical Committee of Peking University School and the Hospital of Stomatology (approval No. PKUSSIRB-2012004). All procedures involving human participants were performed in accordance with relevant guidelines as well as the 1964 Helsinki Declaration and its later amendments or comparable ethical standards.

Mutation Analysis

Extraction of genomic DNA and Sanger sequencing were performed as previously reported [3].

Microcomputed Tomography (microCT) Scanning

In the guided eruption surgery, five pieces of alveolar bone were isolated at random sites of the impacted teeth from the CCD patient. Eight pieces of alveolar bone were collected from three healthy controls. Bone pieces were fixed in 4% paraformaldehyde and scanned by a Siemens Inveon MM Gantry-STD CT (Siemens Medical Solutions, Knoxville, TN, USA). The parameters were as follows: X-ray energy levels of 80 kV, current of 500 µA, and integration time of 1500 ms. Bone mineral density (BMD) was measured using manufacturer-provided software.

Histological Analysis

Alveolar bones were fixed by incubation in 10% buffered formaldehyde for 48 h and decalcified in 10% ethylenedi-amine tetra-acetic acid (EDTA-2Na, pH 7.4) for four weeks with daily replacement. Alveolar bones were embedded in paraffin, and serial Sects. (5 µm) were cut and stained with hematoxylin and eosin or using the Acid Phosphatase Leukocyte (TRAP) Kit (Sigma-Aldrich, MO, USA) according to the manufacturer's instructions. TRAP + osteoclast number was normalized with bone perimeter (N.Oc/B.Pm).

Cell Culture and Osteoclast Differentiation

Mouse macrophage cell line RAW 264.7 cells were maintained in growth medium consisting of DMEM (Gibco, Paisley, UK) and 10% fetal bovine serum (Gibco). Differentiation medium consisted of growth medium supplemented with 10 ng/mL receptor activator of nuclear factor (NF)-κB (RANKL; R&D Systems, USA). Osteoclast differentiation was induced using differentiation medium. Cells were cultured in a humidified incubator with 5% CO_2 at 37 °C.

Lentivirus Construction and Establishment of Stably Infected RAW 264.7 Cells

Lentiviruses containing wild-type RUNX2 (WT-RUNX2) and mutant RUNX2 (c.514delT, p.172 fs; MT-RUNX2) were constructed as previously reported [21]. Lentivirus containing a green fluorescent protein (GFP) tag without a target gene was used as a negative control. Lentiviruses were used to transduce RAW 264.7 cells (multiplicity of infection = 100) in the presence of polybrene (10 µg/mL), and infected cells were selected with puromycin (1 µg/mL). Overexpression of CTSK was performed according to the same method, and a lentivirus containing a GFP tag without CTSK was used as a negative control.

Inhibition and Activation of AKT Phosphorylation

LY294002 (Beyotime Biotechnology, Jiangsu, China), which is a specific PI3K inhibitor, was used at a concentration of 10 µM to block AKT phosphorylation. Overexpression of constitutively active AKT (CA-AKT) or dominant-negative

AKT (DN-AKT) was achieved by infecting cells with lentiviruses. Lentiviruses containing CA-AKT and DN-AKT expression cassettes were constructed by GenePharma Corporation (Shanghai, China).

Real-Time PCR

Total RNA was extracted with TRIzol reagent (Invitrogen, CA, USA). cDNA was generated via reverse transcription with a reverse transcription kit (Thermo Scientific, MA, USA). Real-time PCR was performed using the SYBR Green PCR kit (Roche Applied Science, IN, USA) on the ABI 7500 Real-time PCR System (Applied Biosystems, CA, USA). GAPDH was used as housekeeping gene. Real-time PCR primers were shown in Table 1.

Western Blot

Whole cell lysates were prepared using a RIPA kit (Huaxing Bio, Beijing, China). Nuclear lysates and cytosolic lysates were prepared using the NE-PER™ Nuclear and Cytoplasmic Extraction Reagents (Thermo Scientific). Protein concentrations were quantified with a BCA kit (Thermo Scientific). Protein samples were separated on 10% SDS-PAGE gels and transferred to PVDF membranes (Millipore, MA, USA). Membranes were blocked for 1 h at room temperature in 5% skim milk or BSA and then incubated with primary antibodies overnight at 4 °C. The following primary antibodies were used at a dilution of 1:1,000: RUNX2 (Santa Cruz, CA, USA); GAPHD, β-actin, mTOR (Huaxing Bio); NFATc1, p-mTOR (S2481), Rictor, p-AKT(S473), AKT (CST, MA, USA), c-Fos, and CTSK (Abcam, Cambridge, UK). Secondary antibody coupled to HRP (Jackson ImmunoResearch, PA, USA) was then used (1:10,000 dilution).

Table 1 Primer pairs used in the real-time PCR

Genes	Primer sequences
NFATc1	Forward: 5′-CAGTGTGACCGAAGATACCTGG-3′ Reverse: 5′-TCGAGACTTGATAGGGACCCC-3′
c-Fos	Forward: 5′-CGGCATCATCTAGGCCCAG-3′ Reverse: 5′-TCTGCTGCATAGAAGGAACCG-3′
DC-STAMP	Forward: 5′-GGGGACTTATGTGTTTCCACG-3′ Reverse: 5′-ACAAAGCAACAGACTCCCAAAT-3′
TRAP	Forward: 5′-ACACAGTGATGCTGTGTGGCAACTC-3′ Reverse: 5′-CCAGAGGCTTCCACATATATGATGG-3′
CTSK	Forward: 5′-GAAGAAGACTCACCAGAAGCAG-3′ Reverse: 5′-TCCAGGTTATGGGCAGAGATT-3′
MMP9	Forward: 5′-CTGGACAGCCAGACACTAAAG-3′ Reverse: 5′-CTCGCGGCAAGTCTTCAGAG-3′
GAPDH	Forward: 5′- CGACAGTCAGCCGCATCTT-3′ Reverse: 5′- CCAATACGACCAAATCCGTTG-3′

The immune-reactive bands were detected by an enhanced chemiluminescence blotting kit (Cwbiotech, Jiangsu, China). Blots against GAPDH or β-actin served as a loading control. QuantityOne (Bio-Rad, CA, USA) software was used for densitometric analysis.

Immunofluorescence Staining and Confocal Microscope

RAW 264.7 cells were plated on coverslips at a density of 3×10^4 cells/ml and cultured for certain time and then fixed with 4% paraformaldehyde for 30 min. Cells were permeabilized with 0.5% Triton X-100 for 15 min and blocked with 5% goat serum for 30 min. A RUNX2 antibody or NFATc1 antibody (1:200 dilution) was then added and incubated at 4 °C overnight. Rabbit IgG was used for the negative control. After washing with PBS, cells were incubated with FITC-conjugated secondary antibodies for 30 min at 37 °C. Counterstaining was performed with DAPI to stain nuclei. Confocal images were acquired with a confocal microscope (LMS710, Zeiss, Germany).

Transient Transfection

Briefly, HEK293T cells were plated on coverslips in a 24-well plate at a density of 10^5 cells/well and cultured overnight. Lipofectamine 3000 (Invitrogen, CA, USA) was used to transfect plasmid DNA (500 ng/well) into HEK293T cells following the manufacturer's instruction.

F-Actin Ring Staining

After culture for 5 days with osteoclast differentiation medium, the cells were fixed with 4% paraformaldehyde for 10 min, permeabilized with 0.5% Triton X-100 for 5 min, and washed with PBS. F-actin rings were stained with phalloidin–FITC (Sigma-Aldrich, MO, USA) for 30 min, and cell nuclei were stained with DAPI for 5 min. Images were acquired using a confocal microscope.

TRAP Staining and OCs Counting

RAW 264.7 cells were plated in 24-well plates at a density of 1.5×10^4 cells/well. Cells were cultured for 4 days in differentiation medium. Culture medium was refreshed every 2 days. TRAP staining was processed using a TRAP Kit according to the manufacturer's instruction. Samples were examined using light microscopy (BX51, Olympus, Japan). TRAP + multinucleated cells (three or more nuclei) were counted as osteoclasts.

Bone Resorption Assay

RAW 264.7 cells (1.5×10^4 cells/well) were plated onto Corning Osteo assay Surface in a 24-well plate (Corning, NY, USA), and differentiation medium was refreshed every 2 days. After 7 days, the cells were removed using 10% sodium, and the plate was washed with PBS. Images were captured using light microscopy. Eight random fields per well were recorded, and the area of resorption was measured by Image-Pro Plus 6.0 software (Media Cybernetics, MD, USA).

Statistical Analysis

Results are presented as mean and standard deviation. Student's *t* test and one-way analysis of variance (ANOVA) analyses were performed when appropriate. $p < 0.05$ was considered statistically significant. All experiments were repeated at least three times independently.

Results

Clinical Manifestations and Mutation Analysis of the CCD Patient

The CCD patient showed typical CCD phenotypes, including dental abnormalities (Fig. 1a–c). Two guided eruption surgeries were performed from 2009 to 2019. The panoramic radiograph showed that six permanent teeth were still impacted (15, 13, 25, 23, 34, and 45), and ten supernumerary teeth were present in the premolar regions (Fig. 1d). Our previous study found that this patient has a frameshift mutation (c.514delT, p.172 fs) in the exon 2 of RUNX2 [20] (Fig. 1e), which results in a premature termination codon followed by a truncated RUNX2 protein at a length of 174 amino acids (Fig. 1f). In addition, the 172 fs mutation deletes the entire nuclear localization signal (NLS) domain of the RUNX2 protein, which affects the subcellular location of RUNX2. The truncated RUNX2 protein loses the ability of DNA binding and transcriptional activation.

CCD Patient has Increased Bone Density and Reduced OCs

With regard to the surgically guided eruption of impacted permanent teeth, the alveolar bone around impacted teeth in CCD patients have increased bone density compared with healthy control (systemically healthy subject with delayed eruption teeth). Higher bone density makes it more difficult to remove the obstruction and expose the impacted teeth.

The pieces of removed alveolar bone were gathered in the surgery. Three gender- and age-matched healthy subjects with impacted teeth were used as the control.

MicroCT scanning was performed to acquire the BMD of isolated pieces of alveolar bone from the CCD patient and healthy control. Two-dimensional cross-sectional images showed that, the alveolar bone of the CCD patient was denser than that of the control (Fig. 1g). In addition, the CCD patient had a higher BMD compared to the control (Fig. 1 h, 2322.6 mg/cm^3 vs. 1551.8 mg/cm^3).

Histological analysis and TRAP staining showed TRAP + multinucleated cells in the alveolar bone of the healthy control but not in the CCD patient (Fig. 1i). There was a significant difference in osteoclast number between the healthy control and CCD patient (Fig. 1j). Osteoclasts were not observed in sections from the CCD patient, which may be related to the decreased osteoclast number caused by RUNX2 mutations.

Thus, the RUNX2 mutations may impair OC differentiation and bone remodeling, resulting in delayed permanent teeth eruption in CCD patients.

RUNX2 Promotes OC Differentiation and Bone Resorption

RAW 264.7 cells, which are a classic cell line model for osteoclast study in vitro, were used in the present study. RANKL treatment induced OC differentiation of RAW 264.7 cells intensely (Fig. 2a). Immunofluorescence staining showed that RUNX2 protein was expressed in RAW 264.7 cells and was elevated during RANKL-induced osteoclast differentiation (Fig. 2b). The mRNA and protein expression levels of RUNX2 were constantly increased during OC differentiation of RAW 264.7 cells (Fig. 2c, d), which suggested a potential positive effect of RUNX2 in OC differentiation.

For investigating the effects of RUNX2 mutations on osteoclast differentiation and bone resorption, a lentivirus carrying WT-RUNX2 or MT-RUNX2(172 fs) plasmid was used to infect RAW 264.7 cells. Green fluorescence protein (GFP) was used as a negative control. RUNX2 overexpression was confirmed by real-time PCR and western blot (Fig. 3). Cell lines stably expressing WT-RUNX2 or MT-RUNX2(172 fs) were named as WT-RAW or MT-RAW, respectively. In RANKL-induced OC differentiation, a significantly elevated number of TRAP + multinuclear osteoclasts formed from WT-RAW cells compared with MT-RAW or control cells (Fig. 4a). In addition, WT-RAW cells showed the formation of a well-defined large F-actin ring, representing an increased capability to form sealing zones and to dissolve bone matrix (Fig. 4c). The upregulated bone-resorbing activity of WT-RAW cells was confirmed by a resorption pit assay. On a hydroxyapatite-coated plate, WT-RAW cells formed much
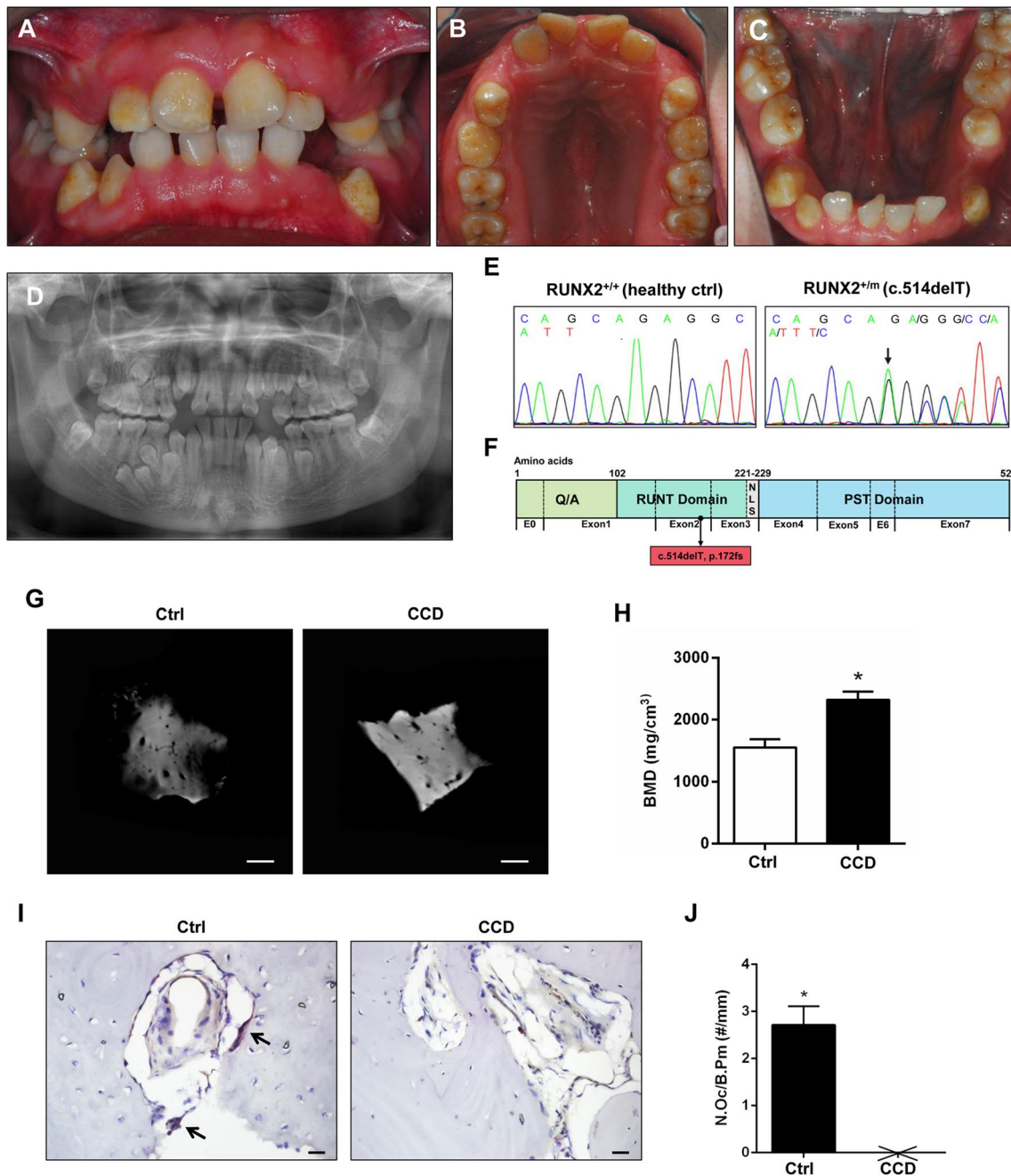
Fig. 1 Manifestations and alveolar bone examination of the CCD patient in the present study. **a-c** Intraoral photographs show retained permanent teeth. **d** Panoramic radiograph shows retained deciduous teeth, delayed eruption of permanent teeth, and supernumerary teeth in the premolar regions. **e** Reverse sequencing data of the RUNX2 gene from the CCD patient and healthy control. Arrows indicated the mutation site. **f** RUNX2 conserved domains and the RUNX2 mutation site in the present study. Q/A, glutamine-/alanine-rich region; RUNT, runt homology domain; NLS, nuclear localization signal; PST, proline/serine/threonine-rich region. **g** Representative microCT images of the isolated alveolar bone from the CCD patient and a healthy control. Scale bar, 1 mm. **h** Quantitative analysis of bone mineral density (BMD). **i** Representative photos of TRAP-stained sections of alveolar bone. Arrows indicate TRAP+osteoclasts (red staining). Scale bar, 20 μm. **j** Quantification of osteoclasts. $*p < 0.05$

larger resorption pits, and the total area of resorptive pits was significantly increased (Fig. 4b). In contrast, mutant RUNX2 had no positive effect on either maturity of OCs or bone resorption. After transient transfection, the GFP control was evenly distributed throughout the cytoplasm and nucleus in HEK293T cells. WT-RUNX2 was located exclusively in the nucleus, while MT-RUNX2 showed impaired nuclear accumulation (Fig. 4d).
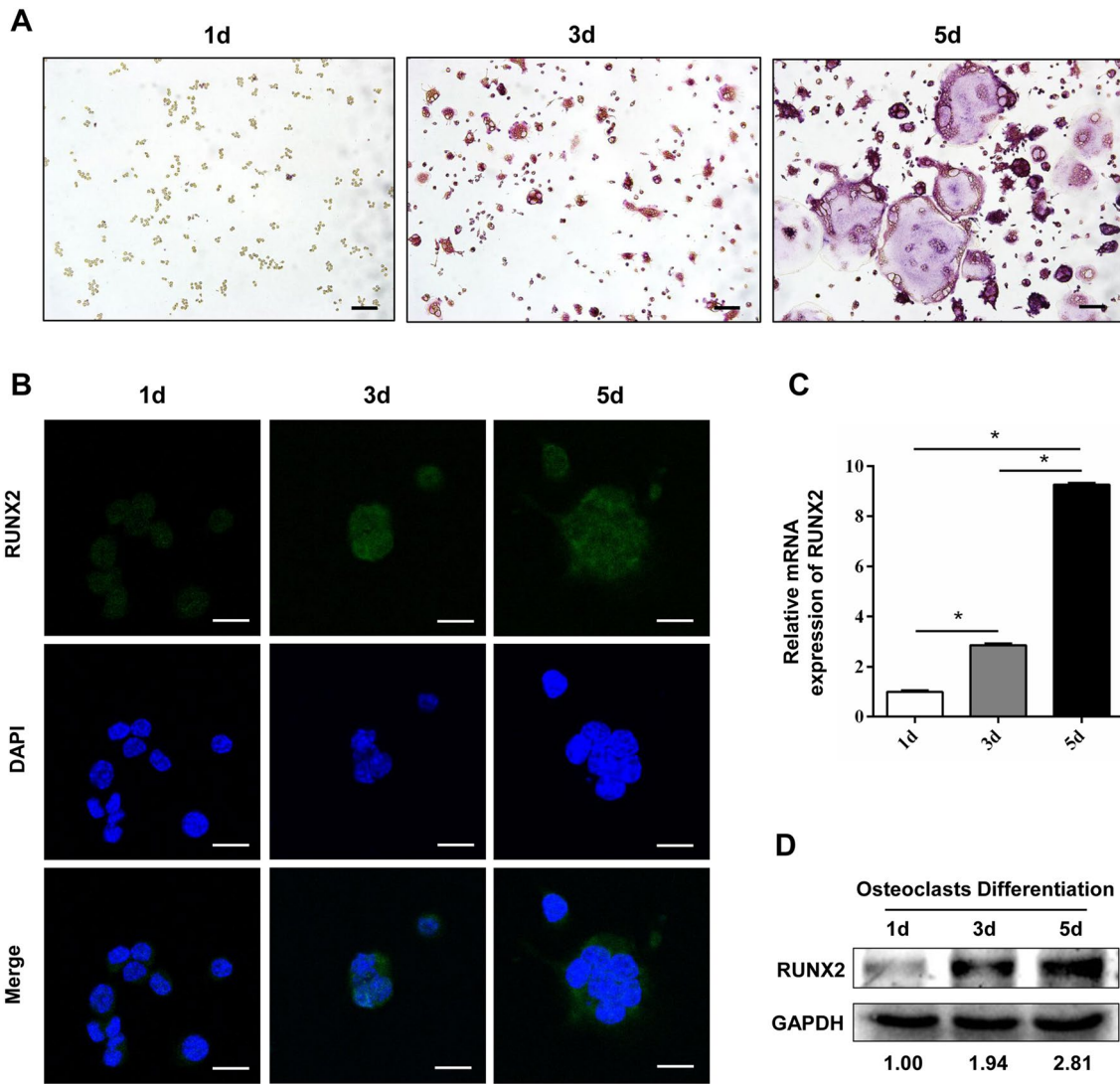
Fig. 2 RUNX2 expressed in RAW 264.7 cells and participated in OC differentiation. a TRAP staining of RAW 264.7 cells in RANKL-induced OC differentiation at indicated time points. Scale bar, 50 μm. b Immunofluorescence detection of RUNX2 in RAW 264.7 cells in OC differentiation. Scale bar, 25 μm. c mRNA expression levels of RUNX2 in RANKL-induced OC differentiation at indicated time points. d Expression levels of RUNX2 protein in RANKL-induced OC differentiation at indicated time points were detected by western blot. *$p < 0.05$
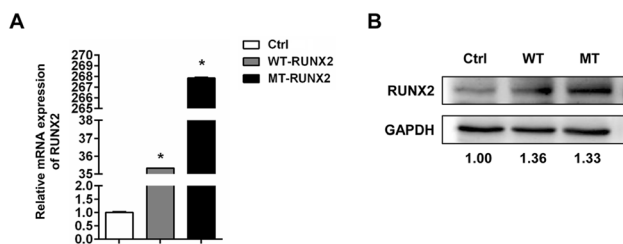
Fig. 3 Establishment of stably overexpressing wild-type (WT) or mutant (MT) RUNX2 RAW 264.7 cell lines. RUNX2 expression was detected at mRNA level by real-time PCR (**a**) and at protein level by western blot (**b**) in the stable cell lines. *$p < 0.05$

Furthermore, mRNA and protein expression levels of genes related to OC formation and bone resorption were assessed. Consistent with the above results, the mRNA levels of genes, including NFATc1, c-Fos, DC-STAMP, TRAP, CTSK, and MMP9, were dramatically increased in WT-RAW cells (Fig. 5a). Western blot results showed that WT-RAW cells expressed higher levels of NFATc1 both in nucleus and cytoplasm (Fig. 5b). The immunofluorescence assay showed that the nuclear translocation of NFATc1 in WT-RAW cells was increased (Fig. 5c). These results suggested that RUNX2 induced the fusion of multinuclear cells, formation of the sealing zone, expression of bone-resorbing protease, and OC differentiation, whereas the mutant
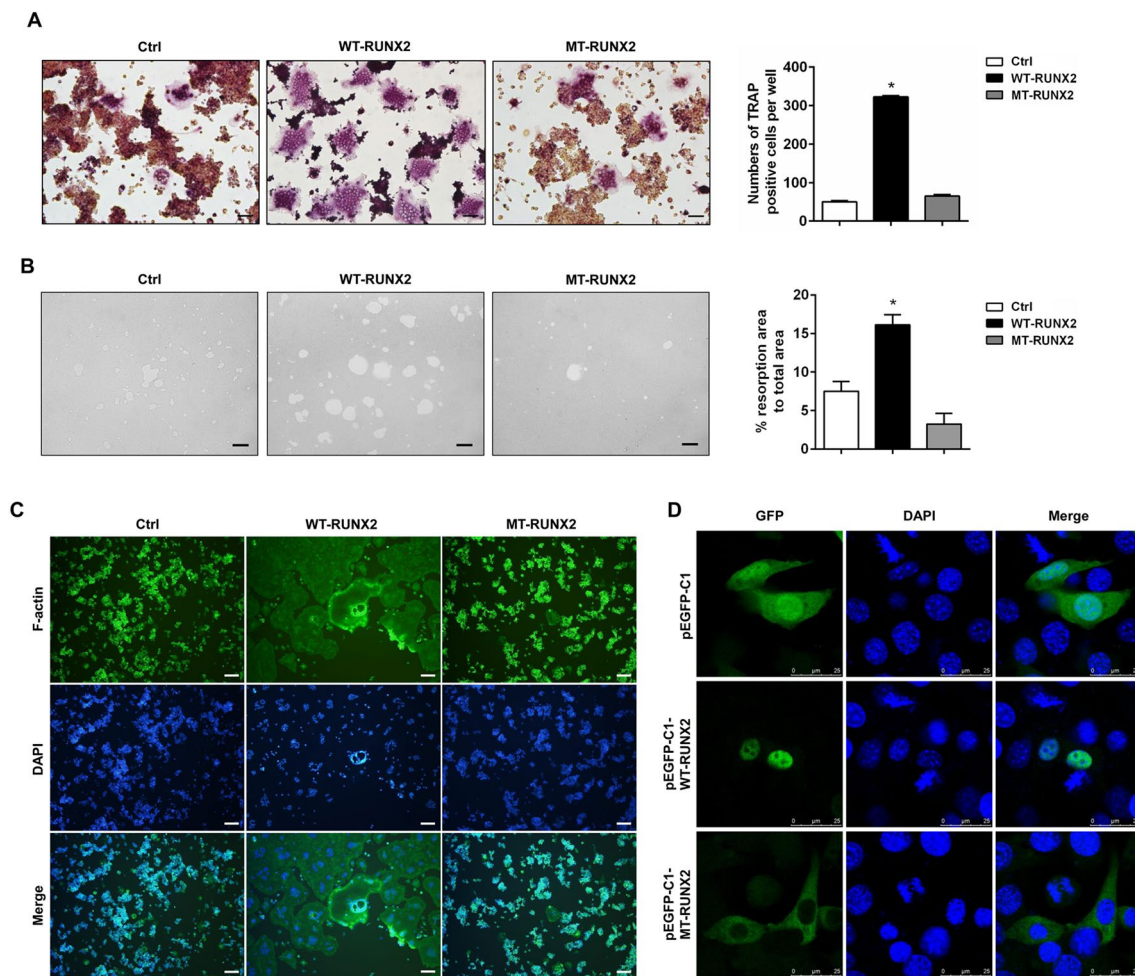
Fig. 4 WT-RUNX2 promoted OC differentiation and function in stable cell lines. **a** After induction with RANKL for 4 days, mature osteoclasts were stained by TRAP. Scale bar, 50 μm. **b** Bone resorption ability of stable cell lines was evaluated by a resorption pit assay. Scale bar, 200 μm. Area of resorption pit was quantified by Image-Pro Plus 6.0 software. **c** Immunofluorescent staining by phalloidin–FITC showed the formation of F-actin rings. Scale bar, 200 μm. **d** Subcellular localization of WT-RUNX2 and MT-RUNX2 was analyzed by immunofluorescence in HEK293T cells. GFP was used as a control. *$p < 0.05$

RUNX2 lost these promoting effects in the entire process of OC differentiation.

RUNX2 Influences Nuclear Translocation of NFATc1 Through Regulating AKT Phosphorylation

The above results showed that NFATc1 levels decreased in MT-RAW cells and that nuclear translocation of NFATc1 was also impacted. Therefore, we assessed the upstream signaling pathway influencing the expression and location of NFATc1. After RANKL treatment, WT-RUNX2 increased the p-AKT(S473) level compared to NC and MT-RUNX2(172 fs) (Fig. 6a).

Because LY294002 suppresses the phosphorylation of AKT by selectively inhibiting PI3K, we compared OC differentiation of WT-RAW cells in the presence or absence of LY294002 to determine if the promoted functions of

WT-RAW cells are related to p-AKT. LY294002(10 μM) sharply reduced p-AKT [Fig. 6b (i)] and resulted in almost complete abrogation of OC formation in WT-RAW cells, and TRAP+multinuclear OCs were significantly decreased and became much smaller [Fig. 6b (ii), (iii)]. NFATc1 and CTSK levels were decreased in the nuclear lysate and whole cell lysate, respectively (Fig. 6c).

We also investigated whether AKT activation rescues the dysfunction of MT-RAW cells [Fig. 6d(i)]. Compared with DN-AKT, overexpression of CA-AKT in MT-RAW cells improved OC differentiation, promoted the nuclear translocation of NFATc1, and increased the expression of CTSK (Fig. 6d, e).

To elucidate the role of enhanced AKT phosphorylation in WT-RAW cells, the activity of mTORC2 was assessed. WT-RAW cells had increased and showed upregulated expression level of p-mTOR(S2481) and Rictor
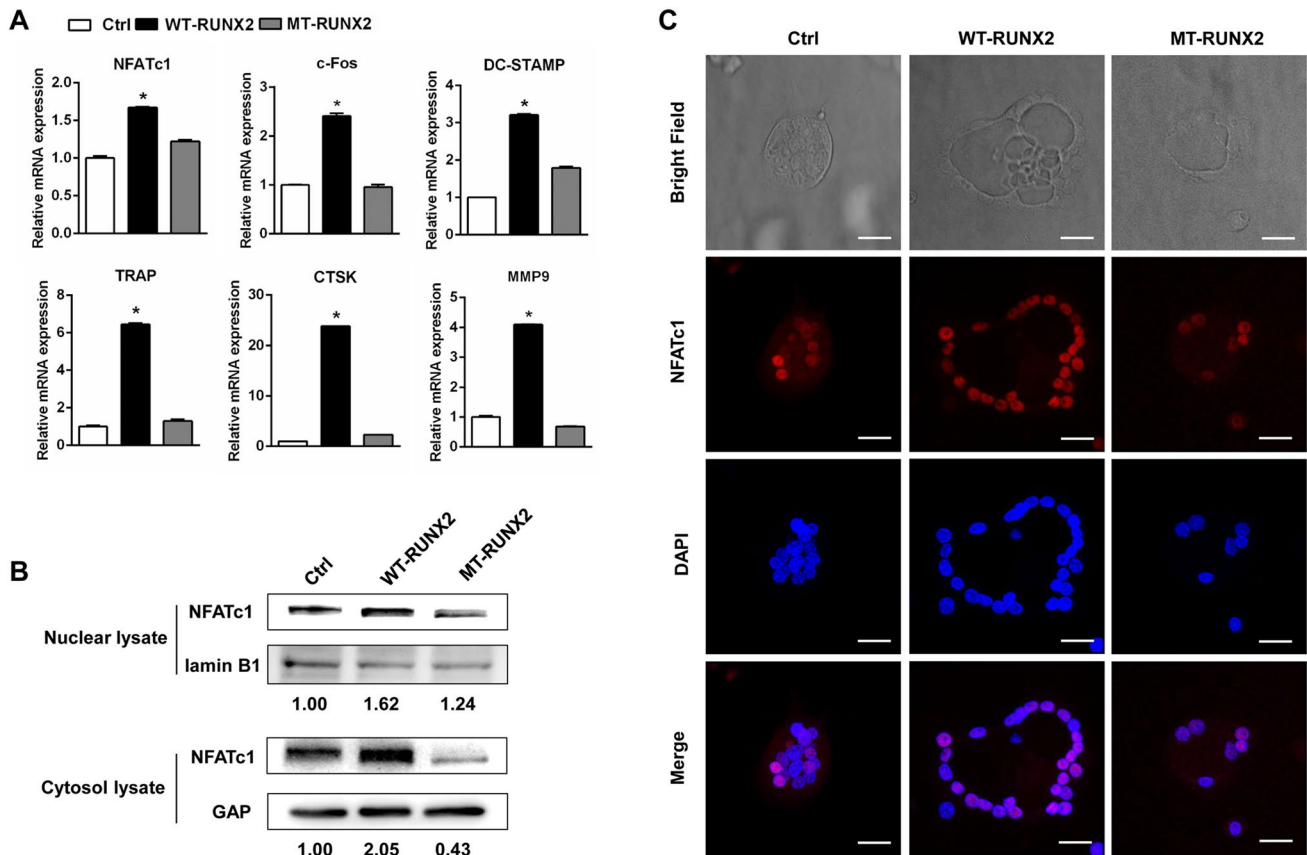
Fig. 5 WT-RUNX2 upregulated the expression of osteoclast-specific genes and promoted nuclear translocation of NFATc1. **a** After induction with RANKL for 3 days, mRNA levels of osteoclast-specific genes in stable cell lines were detected by real-time PCR. **b** Expression levels of NFATc1 were detected by western blot. **c** Confocal microscopy of NFATc1 and nuclei staining in osteoclasts. Scale bar, 25 μm. *$p < 0.05$

(rapamycin-insensitive companion of mTOR), which is a defining component of mTORC2 (Fig. 6f).

Overexpression of CTSK in MT-RAW Partially Rescues OC Functions

Because of the essential function of CTSK in bone resorption, CTSK mRNA was assessed at additional time points. After 3, 5, and 7 days of OC differentiation, the CTSK levels in WT-RAW cells were continuously higher than those in MT-RAW cells (Fig. 7a). To rescue bone-resorbing function of MT-RAW cells, a lentivirus was used to overexpress CTSK in MT-RAW cells, and CTSK protein level was confirmed by western blot (Fig. 7b). CTSK overexpression resulted in the formation of more TRAP + osteoclasts and the increase of bone resorption (Fig. 7c–f). These results indicated that CTSK overexpression partially rescued the differentiation and function of MT-RAW cells to a certain extent.

Discussion

As a typical symptom of CCD, the pathogenesis of delayed eruption of permanent teeth is still far from being fully understood. It is well known that RUNX2 is the master gene of osteogenesis, and deficient osteogenesis is commonly found in RUNX2 mutation-caused CCD patients. Osteogenesis and bone resorption are both involved in the eruption of permanent teeth. Theoretically, if osteogenesis is insufficient and bone resorption is completely unaffected, the BMD of alveolar bone will decrease and the eruption of teeth will be easier. In fact, however, multiple impacted permanent teeth are common in CCD patients. The discrepancy indicated that osteoclast differentiation and function should also be included in the study of the mechanism of the delayed eruption of permanent teeth.

The present study is the first report which finds that RUNX2 mutation-mediated abnormal osteoclast differentiation and deficient bone resorption are involved in
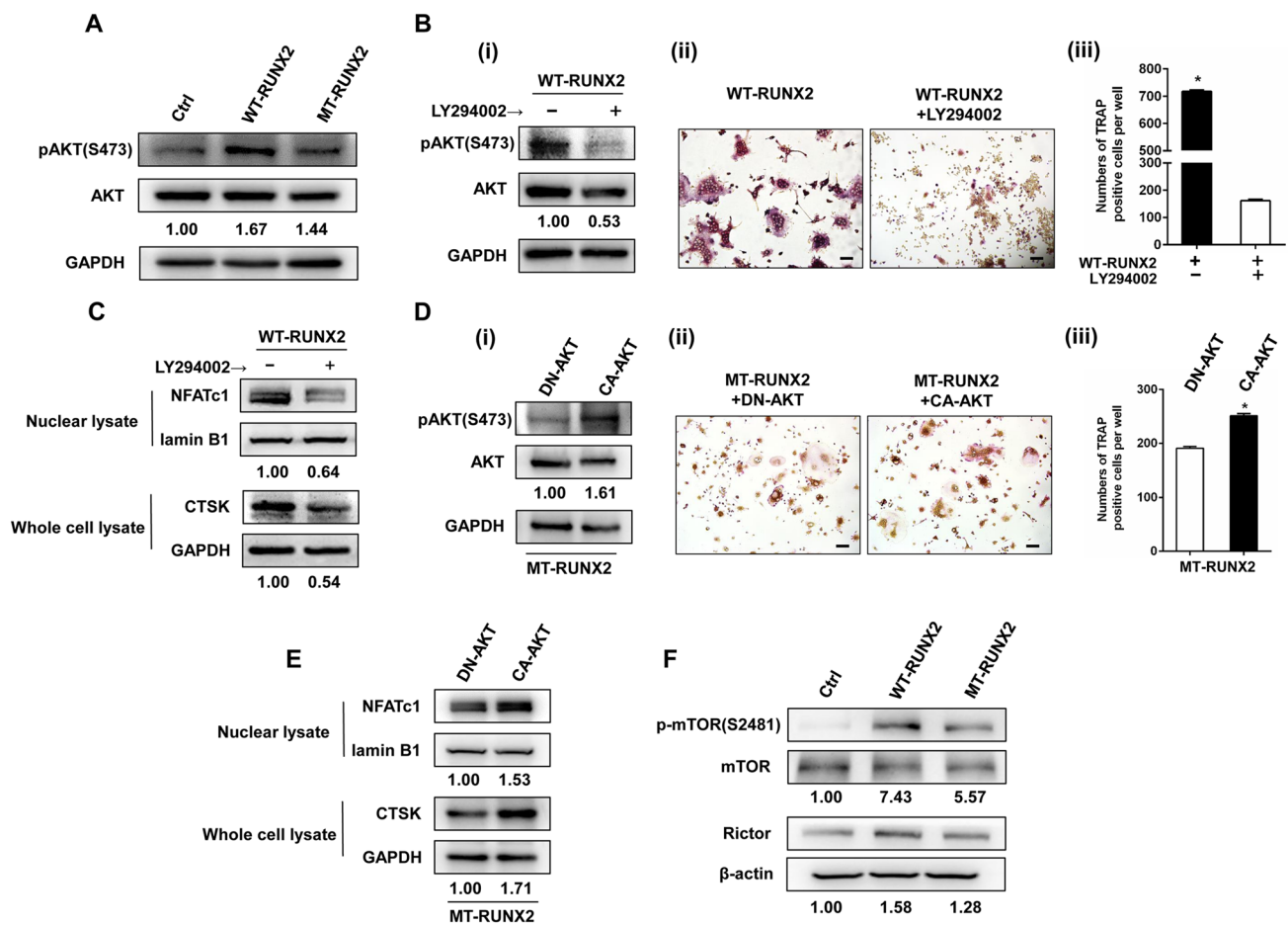
Fig. 6 RUNX2 regulated OC differentiation through the AKT/NFATc1/CTSK axis. **a** WT-RUNX2 increased phosphorylation of AKT(S473) after RANKL treatment for 20 min. **b** LY294002 inhibited AKT phosphorylation (**i**), abrogated OC differentiation (**ii**, **iii**) and decreased NFATc1 and CTSK levels in WT-RAW cells (**c**). **d** CA-AKT in MT-RAW (**i**) promoted OC differentiation(**ii**, **iii**) and increased NFATc1 and CTSK levels (**e**). **f** Phosphorylation of mTOR (S2481) and expression of Rictor were increased in WT-RUNX2 cells after RANKL treatment for 20 min. Scale bar, 50 μm. *$p < 0.05$

defective formation of the tooth eruption pathway and impaction of permanent teeth. Mechanistically, wild-type RUNX2 increased the nuclear accumulation of NFATc1 by promoting AKT phosphorylation. Expression of CTSK was increased by NFATc1, which facilitated bone resorption. However, mutant RUNX2 lost the facilitating functions in osteoclast and bone resorption (Fig. 8).

In the present study, alveolar bone density was increased around the impacted permanent teeth in the CCD patient. Furthermore, osteoclast number was decreased in the local alveolar bone. The anomaly may be directly related to defective formation of the tooth eruption pathway and the impaction of permanent teeth. Osteoporosis, which can be observed in some CCD patients [22], is not indispensable to diagnose CCD [23]. Moreover, BMD was generally evaluated in the spine or long bone [22, 24]; result of alveolar bone has not been reported. However, RUNX2 requirements vary between intramembranous ossification (mandible)

and endochondral ossification (spine and long bone) [25]. Eruption of permanent teeth is more dependent on active bone resorption which may explain why BMD of alveolar bone was increased in CCD patients. When it comes to the impacted permanent teeth in the CCD patients, osteoclasts in alveolar bone should be discussed separately.

By stable expression of WT-RUNX2/MT-RUNX2 in RAW 264.7 cells, we compared OC differentiation and activation of these two stable cell lines. WT-RUNX2 significantly increased the number of TRAP + OCs. WT-RAW cells had more and larger F-actin rings, and bone resorption of WT-RAW cells was also elevated. However, the RUNX2(172 fs) mutant exhibited no positive effect on OCs, which was further verified by subsequent assessment of mRNA and protein levels of OC-specific genes. WT-RUNX2 promoted the expression of osteoclastic genes including NFATc1 and c-Fos (important transcription factors), as well as CTSK and MMP9 (responsible for degradation of bone
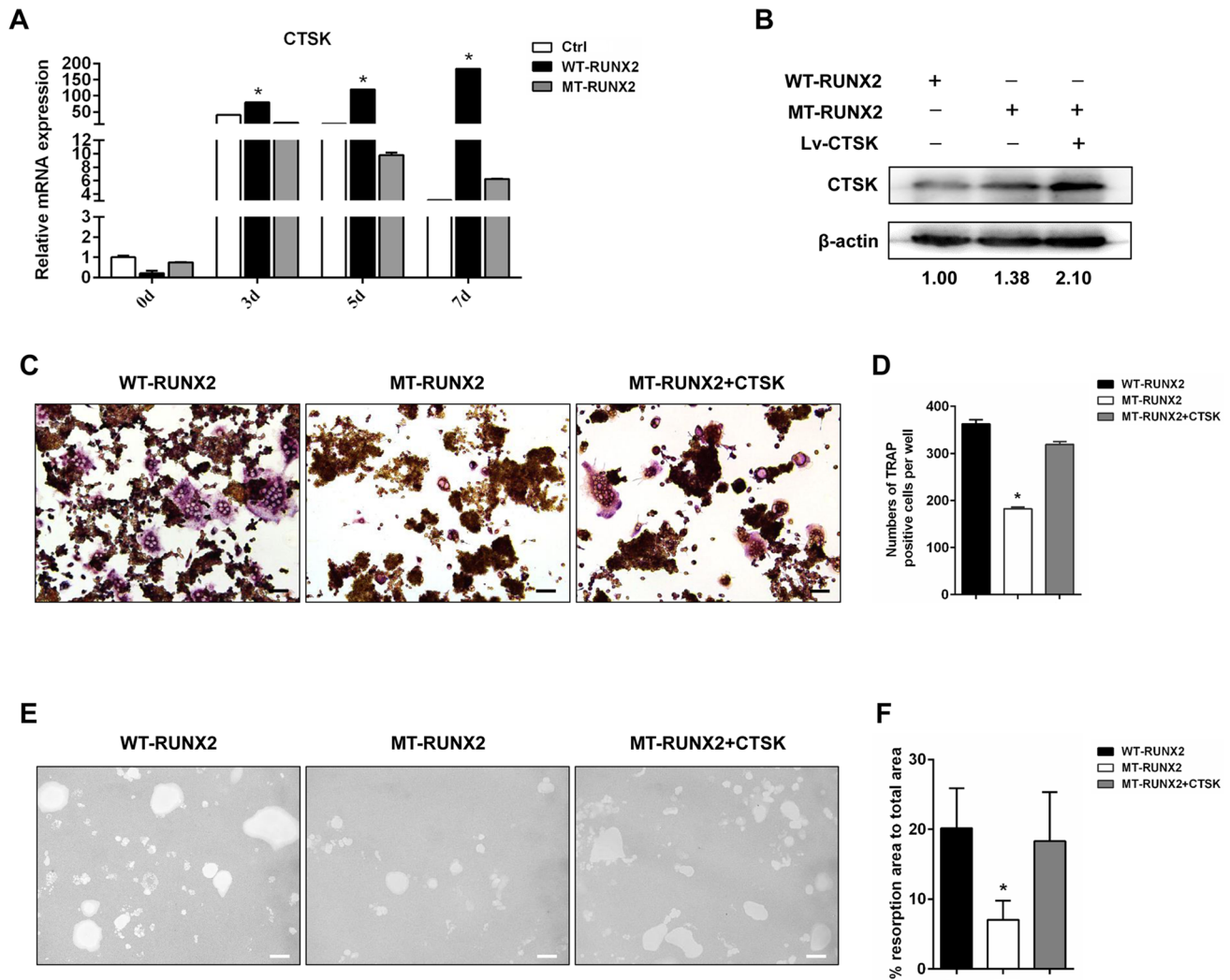
Fig. 7 CTSK overexpression partially rescues OC differentiation and function of MT-RAW cells. **a** mRNA levels of CTSK in stable cell lines with RANKL induction at indicated time points. **b** Overexpression of CTSK detected by western blot. TRAP staining (**c**) and OCs counting (**d**) after CTSK overexpression in MT-RAW cells with RANKL induction. Bone resorption assay (**e**) and quantification of resorption area (**f**) after CTSK overexpression in MT-RAW cells with RANKL induction. Black scale bar, 50 μm. White scale bar, 200 μm. *$p < 0.05$

matrix). These results demonstrated that mutated RUNX2 lost functions in promoting OC differentiation and bone resorption, resulting in decreased OC formation and bone remodeling. This dysfunction may attribute to the defective eruption pathway and delayed permanent tooth eruption in CCD patients.

Subsequently, molecular pathways engaged in OCs regulation were analyzed to further understand RUNX2 function. Playing an indispensable role in the differentiation, maturation, and activation of osteoclasts, NFATc1 directly regulates the expression of several osteoclast-specific genes including TRAP, β3 integrin, CTSK, and MMP9 [26, 27]. As a transcriptional factor, NFATc1 translocates to nucleus and activates downstream genes [28–30]. Activation of

AKT is necessary for the nuclear accumulation of NFATc1 [31]. Sufficient activation of AKT requires phosphorylation at both serine 473 and threonine 308 residues, which rely on phosphatidylinositol-dependent kinase 1 (PDK1) and mammalian target of rapamycin complex-2 (mTORC2), respectively [32]. Glycogen synthase kinase-3β (GSK3β) interferes with osteoclast differentiation by the nuclear export of NFATc1 [33, 34]. Activated AKT phosphorylates GSK3β at the serine residue, thereby removing the blockage on NFATc1 translocation [31]. In RANKL-induced differentiation, the p-AKT (S473) level was elevated in WT-RAW cells compared with MT-RAW cells, which subsequently promoted the nuclear accumulation of NFATc1. LY294002 reduced AKT phosphorylation (S473) in WT-RAW cells and
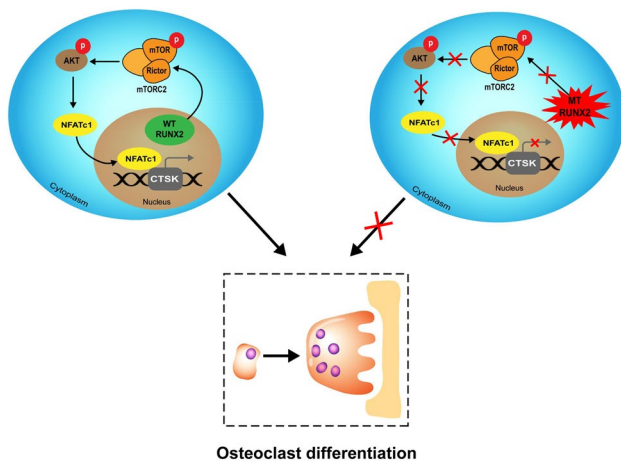
Fig. 8 Schematic representation of the AKT/NFATc1/CTSK axis regulated by RUNX2 in the process of osteoclast differentiation. Wild-type RUNX2 increased expression and activity of mTORC2, which promoted AKT(S473) phosphorylation. Elevated p-AKT subsequently increased nuclear translocation of NFATc1 and CTSK expression. Mutant RUNX2 lost the facilitating function on osteoclasts

even almost completely abrogated OC differentiation. A few small TRAP + OCs were observed and the expression levels of NFATc1 and CTSK were also significantly decreased. Interestingly, when the serine 473 residue of AKT was constitutively phosphorylated, the impaired OC formation of MT-RAW cells was rescued, and the nuclear translocation of NFATc1 and the expression of CTSK were increased. Therefore, RUNX2 may mediate the nuclear translocation of NFATc1 by upregulating AKT phosphorylation, thereby improving OC fusion, activation, and bone-resorbing function.

To investigate the mechanism of increased p-AKT(S473) by wild-type RUNX2, we evaluated the phosphorylation of mTOR and the expression level of Rictor, which is a specific component of mTORC2. mTOR phosphorylation at the serine 2481 residue and Rictor expression were increased in WT-RAW cells. Ser2481 phosphorylation is specific for mTORC2 and can be used as a biomarker for intact mTORC2 [35]. Furthermore, Rictor levels have been reported to be positively correlated with mTORC2 activity [36, 37]. Therefore, both p-mTOR (S2481) and Rictor elevated the activity of mTORC2 in WT-RAW cells. RUNX2 could be recruited on mTOR promoter and the expression of Rictor was RUNX2-dependent [38] so that overexpression of wild-type RUNX2 increased mTORC2 activity. However, consistent with our previous study [20], mutant RUNX2 could not accumulate in the nucleus, which resulted in decreased mTORC2 expression and activity.

CTSK, which is a key member of the downstream genes of NFATc1, plays a critical role in bone resorption [39]. It should be noticed that CTSK participates in regulating the apoptosis and senescence of OCs [40] beyond just bone matrix degradation. CTSK also influences the ultrastructure of ruffled borders [41], which is related to efficiency of bone resorption. CTSK$^{-/-}$ mice exhibit a human pycnodysostosis-like phenotype, and CTSK$^{-/-}$ OCs shows impaired apoptosis and senescence [40]. Inhibitors of CTSK have been used in the treatment of osteoporosis [42]. In the present study, CTSK was robustly upregulated by WT-RUNX2 in OC differentiation (Fig. 5s, 7a). Considering the multiple functions and expression level, CTSK was used as the target in the rescue of the bone-resorbing function of osteoclasts with RUNX2 mutation. Lentiviral transduction of CTSK into mutated RAW 264.7 cells partially rescued OC differentiation and bone resorption. These results suggested the potential effect of CTSK in improving bone remodeling and formation of the eruption pathway in CCD patients. Local application of exogenous CTSK may be considered as a method to promote normal tooth eruption in CCD patients.

Inorganic hydroxyapatite is the main composition of bone and the dissolution of hydroxyapatite is a crucial step in bone resorption. Organic compositions including collagen and glycoprotein will also be degraded once the inorganic scaffold is destroyed. Hydroxyapatite-coated plate (Osteo Assay plate) has been used in the studies of bone resorption [43, 44], but dentin slices or bone slices should be used in the study focusing on the degradation of organic compositions.

To date, only two articles reported the relationship between RUNX2 gene deficiency and osteoclast differentiation. Faienza et al. [45] isolated peripheral blood mononuclear cells (PBMCs) from a 4-year-old child who has been diagnosed as CCD. They reported that a complete heterozygous RUNX2 deletion did not affect osteoclastogenesis. Another paper [46] showed that active alveolar bone resorption is limited in heterozygous Runx2 knockout mice, which leads to the delay of tooth eruption. The discrepancy indicates that RUNX2 mutation may play a different role from heterozygous RUNX2 deletion in the process of osteoclastogenesis, which further supports our conclusion derived from this study.

RAW 264.7 cells have been extensively employed in the study of OC differentiation and function [47–49]. As a previous study reported [50], compared with RAW 264.7 cells, the efficiency of gene transduction into primary bone marrow cells is low. We have tried to transduce wild-type RUNX2 and mutant RUNX2 into primary bone marrow cells, but the result was unsatisfactory and was influenced by many external factors (data not shown). In consideration of the differences between RAW 264.7 cells and primary bone marrow cells, in further study, gene editing mouse with RUNX2 mutation (c.514delT, p.172 fs) should be generated. Primary bone marrow cells should be isolated from the gene

editing mouse and then be used to confirm the function of RUNX2 in osteoclast.

In conclusion, the present study reports for the first time that RUNX2 regulates osteoclast differentiation and bone resorption. Wild-type RUNX2 promotes the formation of tooth eruption pathway through the AKT/NFATc1/CTSK axis. In the CCD patient, mutant RUNX2 lost the facilitating functions on osteoclasts, resulting in the retention of deciduous teeth and the impaction of permanent teeth. This study further illustrates the mechanism of delayed eruption of permanent teeth in CCD in terms of the dysfunction of osteoclasts.

Author Contributions Conceptualization: YX, YW and SZ; Methodology: YX, DL, JL and CZ; Data Curation: YX and YL; Writing—Original Draft Preparation: YX; Writing—Review & Editing: YW and SZ.

Compliance with Ethical Standards

Conflict of interest Yuejiao Xin, Yang Liu, Dandan Liu, Jie Li, Chenying Zhang, Yixiang Wang, and Shuguo Zheng declare that they have no conflict of interest.

Human and Animal Rights and Informed Consent This study was approved by the Ethical Committee of Peking University School and the Hospital of Stomatology (Approval No. PKUSSIRB-2012004) and conducted strictly in accordance with the 1964 Helsinki Declaration and its later amendments or comparable ethical standards. All participants signed an informed consent prior to study.

References

1. Ott CE, Leschik G, Trotier F, Brueton L, Brunner HG, Brussel W, Guillen-Navarro E, Haase C, Kohlhase J, Kotzot D, Lane A, Lee-Kirsch MA, Morlot S, Simon ME, Steichen-Gersdorf E, Tegay DH, Peters H, Mundlos S, Klopocki E (2010) Deletions of the RUNX2 gene are present in about 10% of individuals with cleidocranial dysplasia. Hum Mutat 31(8):E1587–1593. https://doi.org/10.1002/humu.21298

2. Cooper SC, Flaitz CM, Johnston DA, Lee B, Hecht JT (2001) A natural history of cleidocranial dysplasia. Am J Med Genet 104(1):1–6

3. Zhang CY, Zheng SG, Wang YX, Zhu JX, Zhu X, Zhao YM, Ge LH (2009) Novel RUNX2 mutations in Chinese individuals with cleidocranial dysplasia. J Dental Res 88(9):861–866. https://doi.org/10.1177/0022034509342083

4. Jaruga A, Hordyjewska E, Kandzierski G, Tylzanowski P (2016) Cleidocranial dysplasia and RUNX2-clinical phenotype-genotype correlation. Clin Genet 90(5):393–402. https://doi.org/10.1111/cge.12812

5. Wise GE (2009) Cellular and molecular basis of tooth eruption. Orthod Cranio Res 12(2):67–73. https://doi.org/10.1111/j.1601-6343.2009.01439.x

6. Wise GE, He H, Gutierrez DL, Ring S, Yao S (2011) Requirement of alveolar bone formation for eruption of rat molars. Eur J Oral Sci 119(5):333–338. https://doi.org/10.1111/j.1600-0722.2011.00854.x

7. Wise GE, Yao S (2006) Regional differences of expression of bone morphogenetic protein-2 and RANKL in the rat dental follicle. Eur J Oral Sci 114(6):512–516. https://doi.org/10.1111/j.1600-0722.2006.00406.x

8. Castaneda B, Simon Y, Jacques J, Hess E, Choi YW, Blin-Wakkach C, Mueller C, Berdal A, Lezot F (2011) Bone resorption control of tooth eruption and root morphogenesis: involvement of the receptor activator of NF-kappaB (RANK). J Cell Physiol 226(1):74–85. https://doi.org/10.1002/jcp.22305

9. Wise GE, Yao S, Henk WG (2007) Bone formation as a potential motive force of tooth eruption in the rat molar. Clin Anat 20(6):632–639. https://doi.org/10.1002/ca.20495

10. Takarada T, Hinoi E, Nakazato R, Ochi H, Xu C, Tsuchikane A, Takeda S, Karsenty G, Abe T, Kiyonari H, Yoneda Y (2013) An analysis of skeletal development in osteoblast-specific and chondrocyte-specific runt-related transcription factor-2 (Runx2) knockout mice. J Bone Miner Res 28(10):2064–2069. https://doi.org/10.1002/jbmr.1945

11. Chen P, Wei D, Xie B, Ni J, Xuan D, Zhang J (2014) Effect and possible mechanism of network between microRNAs and RUNX2 gene on human dental follicle cells. J Cell Biochem 115(2):340–348. https://doi.org/10.1002/jcb.24668

12. Yan WJ, Zhang CY, Yang X, Liu ZN, Wang XZ, Sun XY, Wang YX, Zheng SG (2015) Abnormal differentiation of dental pulp cells in cleidocranial dysplasia. J Dental Res 94(4):577–583. https://doi.org/10.1177/0022034514566655

13. Udagawa N, Takahashi N, Akatsu T, Tanaka H, Sasaki T, Nishihara T, Koga T, Martin TJ, Suda T (1990) Origin of osteoclasts: mature monocytes and macrophages are capable of differentiating into osteoclasts under a suitable microenvironment prepared by bone marrow-derived stromal cells. Proc Natl Acad Sci USA 87(18):7260–7264. https://doi.org/10.1073/pnas.87.18.7260

14. Lacey DL, Timms E, Tan HL, Kelley MJ, Dunstan CR, Burgess T, Elliott R, Colombero A, Elliott G, Scully S, Hsu H, Sullivan J, Hawkins N, Davy E, Capparelli C, Eli A, Qian YX, Kaufman S, Sarosi I, Shalhoub V, Senaldi G, Guo J, Delaney J, Boyle WJ (1998) Osteoprotegerin ligand is a cytokine that regulates osteoclast differentiation and activation. Cell 93(2):165–176

15. Yasuda H, Shima N, Nakagawa N, Yamaguchi K, Kinosaki M, Mochizuki S, Tomoyasu A, Yano K, Goto M, Murakami A, Tsuda E, Morinaga T, Higashio K, Udagawa N, Takahashi N, Suda T (1998) Osteoclast differentiation factor is a ligand for osteoprotegerin/osteoclastogenesis-inhibitory factor and is identical to TRANCE/RANKL. Proc Natl Acad Sci USA 95(7):3597–3602. https://doi.org/10.1073/pnas.95.7.3597

16. Suda T, Takahashi N, Udagawa N, Jimi E, Gillespie MT, Martin TJ (1999) Modulation of osteoclast differentiation and function by the new members of the tumor necrosis factor receptor and ligand families. Endocr Rev 20(3):345–357. https://doi.org/10.1210/edrv.20.3.0367

17. Enomoto H, Shiojiri S, Hoshi K, Furuichi T, Fukuyama R, Yoshida CA, Kanatani N, Nakamura R, Mizuno A, Zanma A, Yano K, Yasuda H, Higashio K, Takada K, Komori T (2003) Induction of osteoclast differentiation by Runx2 through receptor activator of nuclear factor-kappa B ligand (RANKL) and osteoprotegerin regulation and partial rescue of osteoclastogenesis in Runx2-/- mice by RANKL transgene. J Biol Chem 278(26):23971–23977. https://doi.org/10.1074/jbc.M302457200

18. Martin A, Xiong J, Koromila T, Ji JS, Chang S, Song YS, Miller JL, Han CY, Kostenuik P, Krum SA, Chimge NO, Gabet Y, Frenkel B (2015) Estrogens antagonize RUNX2-mediated osteoblast-driven osteoclastogenesis through regulating RANKL

membrane association. Bone 75:96–104. https://doi.org/10.1016/j.bone.2015.02.007

19. Byon CH, Sun Y, Chen J, Yuan K, Mao X, Heath JM, Anderson PG, Tintut Y, Demer LL, Wang D, Chen Y (2011) Runx2-upregulated receptor activator of nuclear factor kappaB ligand in calcifying smooth muscle cells promotes migration and osteoclastic differentiation of macrophages. Arterioscler Thromb Vasc Biol 31(6):1387–1396. https://doi.org/10.1161/atvbaha.110.222547

20. Zhang C, Zheng S, Wang Y, Zhao Y, Zhu J, Ge L (2010) Mutational analysis of RUNX2 gene in Chinese patients with cleidocranial dysplasia. Mutagenesis 25(6):589–594. https://doi.org/10.1093/mutage/geq044

21. Liu Y, Sun X, Zhang X, Wang X, Zhang C, Zheng S (2019) RUNX2 mutation impairs osteogenic differentiation of dental follicle cells. Arch Oral Biol 97:156–164. https://doi.org/10.1016/j.archoralbio.2018.10.029

22. Dincsoy Bir F, Dinckan N, Guven Y, Bas F, Altunoglu U, Kuvvetli SS, Poyrazoglu S, Toksoy G, Kayserili H, Uyguner ZO (2017) Cleidocranial dysplasia: clinical, endocrinologic and molecular findings in 15 patients from 11 families. Eur J Med Genet 60(3):163–168. https://doi.org/10.1016/j.ejmg.2016.12.007

23. Mundlos S (1999) Cleidocranial dysplasia: clinical and molecular genetics. J Med Genet 36(3):177–182

24. Bergwitz C, Prochnau A, Mayr B, Kramer FJ, Rittierodt M, Berten HL, Hausamen JE, Brabant G (2001) Identification of novel CBFA1/RUNX2 mutations causing cleidocranial dysplasia. J Inherit Metab Dis 24(6):648–656. https://doi.org/10.1023/a:1012758925617

25. Yoshida T, Kanegane H, Osato M, Yanagida M, Miyawaki T, Ito Y, Shigesada K (2002) Functional analysis of RUNX2 mutations in Japanese patients with cleidocranial dysplasia demonstrates novel genotype-phenotype correlations. Am J Hum Genet 71(4):724–738. https://doi.org/10.1086/342717

26. Song I, Kim JH, Kim K, Jin HM, Youn BU, Kim N (2009) Regulatory mechanism of NFATc1 in RANKL-induced osteoclast activation. FEBS Lett 583(14):2435–2440. https://doi.org/10.1016/j.febslet.2009.06.047

27. Asagiri M, Takayanagi H (2007) The molecular understanding of osteoclast differentiation. Bone 40(2):251–264. https://doi.org/10.1016/j.bone.2006.09.023

28. Lu SY, Li M, Lin YL (2014) Mitf regulates osteoclastogenesis by modulating NFATc1 activity. Exp Cell Res 328(1):32–43. https://doi.org/10.1016/j.yexcr.2014.08.018

29. Matsumoto M, Kogawa M, Wada S, Takayanagi H, Tsujimoto M, Katayama S, Hisatake K, Nogi Y (2004) Essential role of p38 mitogen-activated protein kinase in cathepsin K gene expression during osteoclastogenesis through association of NFATc1 and PU.1. J Biol Chem 279 (44):45969–45979. https://doi.org/10.1074/jbc.M408795200

30. Matsuo K, Galson DL, Zhao C, Peng L, Laplace C, Wang KZ, Bachler MA, Amano H, Aburatani H, Ishikawa H, Wagner EF (2004) Nuclear factor of activated T-cells (NFAT) rescues osteoclastogenesis in precursors lacking c-Fos. J Biol Chem 279(25):26475–26480. https://doi.org/10.1074/jbc.M313973200

31. Moon JB, Kim JH, Kim K, Youn BU, Ko A, Lee SY, Kim N (2012) Akt induces osteoclast differentiation through regulating the GSK3beta/NFATc1 signaling cascade. J Immunol 188(1):163–169. https://doi.org/10.4049/jimmunol.1101254

32. Bhaskar PT, Hay N (2007) The two TORCs and Akt. Dev Cell 12(4):487–502. https://doi.org/10.1016/j.devcel.2007.03.020

33. Wu M, Chen W, Lu Y, Zhu G, Hao L, Li YP (2017) Galpha13 negatively controls osteoclastogenesis through inhibition of the Akt-GSK3beta-NFATc1 signalling pathway. Nat Commun 8:13700. https://doi.org/10.1038/ncomms13700

34. Jang HD, Shin JH, Park DR, Hong JH, Yoon K, Ko R, Ko CY, Kim HS, Jeong D, Kim N, Lee SY (2011) Inactivation of glycogen synthase kinase-3beta is required for osteoclast differentiation. J Biol Chem 286(45):39043–39050. https://doi.org/10.1074/jbc.M111.256768

35. Copp J, Manning G, Hunter T (2009) TORC-specific phosphorylation of mammalian target of rapamycin (mTOR): phospho-Ser2481 is a marker for intact mTOR signaling complex 2. Cancer Res 69(5):1821–1827. https://doi.org/10.1158/0008-5472.can-08-3014

36. Masri J, Bernath A, Martin J, Jo OD, Vartanian R, Funk A, Gera J (2007) mTORC2 activity is elevated in gliomas and promotes growth and cell motility via overexpression of rictor. Cancer Res 67(24):11712–11720. https://doi.org/10.1158/0008-5472.can-07-2223

37. Huang S, Yang ZJ, Yu C, Sinicrope FA (2011) Inhibition of mTOR kinase by AZD8055 can antagonize chemotherapy-induced cell death through autophagy induction and down-regulation of p62/sequestosome 1. J Biol Chem 286(46):40002–40012. https://doi.org/10.1074/jbc.M111.297432

38. Tandon M, Chen Z, Pratap J (2014) Runx2 activates PI3K/Akt signaling via mTORC2 regulation in invasive breast cancer cells. Breast Cancer Res 16(1):R16. https://doi.org/10.1186/bcr3611

39. Lotinun S, Kiviranta R, Matsubara T, Alzate JA, Neff L, Luth A, Koskivirta I, Kleuser B, Vacher J, Vuorio E, Horne WC, Baron R (2013) Osteoclast-specific cathepsin K deletion stimulates S1P-dependent bone formation. J Clin Investig 123(2):666–681. https://doi.org/10.1172/jci64840

40. Chen W, Yang S, Abe Y, Li M, Wang Y, Shao J, Li E, Li YP (2007) Novel pycnodysostosis mouse model uncovers cathepsin K function as a potential regulator of osteoclast apoptosis and senescence. Hum Mol Genet 16(4):410–423. https://doi.org/10.1093/hmg/ddl474

41. Saftig P, Hunziker E, Wehmeyer O, Jones S, Boyde A, Rommerskirch W, Moritz JD, Schu P, von Figura K (1998) Impaired osteoclastic bone resorption leads to osteopetrosis in cathepsin-K-deficient mice. Proc Natl Acad Sci USA 95(23):13453–13458. https://doi.org/10.1073/pnas.95.23.13453

42. Panwar P, Soe K, Guido RV, Bueno RV, Delaisse JM, Bromme D (2016) A novel approach to inhibit bone resorption: exosite inhibitors against cathepsin K. Br J Pharmacol 173(2):396–410. https://doi.org/10.1111/bph.13383

43. Prates TP, Taira TM, Holanda MC, Bignardi LA, Salvador SL, Zamboni DS, Cunha FQ, Fukada SY (2014) NOD2 contributes to Porphyromonas gingivalis-induced bone resorption. J Dental Res 93(11):1155–1162. https://doi.org/10.1177/0022034514551770

44. Sharmin F, McDermott C, Lieberman J, Sanjay A, Khan Y (2017) Dual growth factor delivery from biofunctionalized allografts: Sequential VEGF and BMP-2 release to stimulate allograft remodeling. J Orthop Res 35(5):1086–1095. https://doi.org/10.1002/jor.23287

45. Faienza MF, Ventura A, Piacente L, Ciccarelli M, Gigante M, Gesualdo L, Colucci S, Cavallo L, Grano M, Brunetti G (2014) Osteoclastogenic potential of peripheral blood mononuclear cells in cleidocranial dysplasia. Int J Med Sci 11(4):356–364. https://doi.org/10.7150/ijms.7793

46. Yoda S, Suda N, Kitahara Y, Komori T, Ohyama K (2004) Delayed tooth eruption and suppressed osteoclast number in the eruption pathway of heterozygous Runx2/Cbfa1 knockout mice. Arch Oral Biol 49(6):435–442. https://doi.org/10.1016/j.archoralbio.2004.01.010

47. Collin-Osdoby P, Osdoby P (2012) RANKL-mediated osteoclast formation from murine RAW 264.7 cells. Methods Mol Biol 816:187–202. https://doi.org/10.1007/978-1-61779-415-5_13

48. Laha D, Deb M, Das H (2019) KLF2 (kruppel-like factor 2 [lung]) regulates osteoclastogenesis by modulating autophagy. Autophagy 15(12):2063–2075. https://doi.org/10.1080/15548627.2019.1596491

49. Hao S, Meng J, Zhang Y, Liu J, Nie X, Wu F, Yang Y, Wang C, Gu N, Xu H (2017) Macrophage phenotypic mechanomodulation of enhancing bone regeneration by superparamagnetic scaffold upon magnetization. Biomaterials 140:16–25. https://doi.org/10.1016/j.biomaterials.2017.06.013

50. Yamamoto A, Miyazaki T, Kadono Y, Takayanagi H, Miura T, Nishina H, Katada T, Wakabayashi K, Oda H, Nakamura K, Tanaka S (2002) Possible involvement of IkappaB kinase 2 and MKK7 in osteoclastogenesis induced by receptor activator of nuclear factor kappaB ligand. J Bone Miner Res 17(4):612–621. https://doi.org/10.1359/jbmr.2002.17.4.612